THE JOURNAL OF PHYSICAL CHEMISTRY A LETTERS

2005, *109,* 8443−8446
Published on Web 08/31/2005

Theoretical Study toward Understanding Ultrafast Internal Conversion of Excited 9H-Adenine

Hui Chen and Shuhua Li*

Department of Chemistry, Institute of Theoretical and Computational Chemistry, Lab of Mesoscopic Chemistry, Nanjing University, Nanjing, 210093, P. R. China

Received: July 7, 2005

The CASPT2/CASSCF method with the 6-311G* basis set and an active space up to (14, 11) was used to explore the ultrafast internal conversion mechanism for excited 9H-adenine. Three minima, two transition states, and seven conical intersections were obtained to build up the two deactivation pathways for the internal conversion mechanism. Special efforts were made to explore the excited-state potential energy surfaces near the Franck−Condon region and determine the various barriers in the processes of deactivation. The barrier required from the $^1\pi\pi^*$ (^1L_a) state to deactivate nonradiatively is found to be lower than that required from the $^1\pi\pi^*$ (^1L_b) state. On 250 nm excitation, the $^1\pi\pi^*$ (^1L_a) state is populated, and the transition from $^1\pi\pi^*$ (^1L_a) to the lowest $^1n\pi^*$ state involves very low barriers, which may account for the observed short (<50 fs) lifetime of the $^1\pi\pi^*$ excited state. The deactivation of the lowest $^1n\pi^*$ state is required to overcome a barrier of 3.15 kcal/mol, which should be responsible for the 750 fs lifetime of the $n\pi^*$ excited state. On 267 nm excitation, the vibrationally active $^1\pi\pi^*$ (^1L_b) state is populated. Excitation at 277 nm prepares the $^1\pi\pi^*$ (^1L_b) state without much excessive vibrational energy, which may be responsible for the observed >2 ps lifetime.

As the most important building blocks of the genetic material of life, the nucleobases in DNA/RNA have demonstrated a high degree of photostability, which can protect life from the DNA/RNA photochemical damage from the UV irradiation of sunlight.[1,2] The DNA/RNA nucleosides, nucleotides in solvent, and isolated purine and pyrimidine bases in the gas phase all exhibit short excited-state lifetimes (picoseconds) at room temperature.[1−9] It seems that the ultrafast nonradiative deactivation of excited nucleobases back to the ground state to avoid photochemical reactions is the intrinsic property of these molecules. An ultrafast internal conversion is proposed for the ultrafast nonradiative deactivation.[3,4] As shown in the theoretical study of cytosine, the conical intersection (CI) is found to account for the ultrafast internal conversion.[10,11]

Recently, a theoretical work[12] performed at the CASSCF/6-31G** level with a relatively small active space (6, 6) led to two S_1/S_0 CIs, which were proposed to be responsible for the ultrafast internal conversion of excited 9H-adenine. The calculated results show that these two CIs arise from $^1\pi\pi^*(L_a)-S_0$ and $^1n\pi^*-S_0$ diabatic state crossings, respectively. The $\pi\pi^*/S_0$ CI was also confirmed by other authors with a different computational method.[13] Although this work has shed some light on the mechanism of the ultrafast internal conversion in excited 9H-adenine, there are still many unknown aspects to be explored. For example, we have little knowledge on excited-state potential energy surfaces near the Franck−Condon region. On the other hand, although various barriers in two deactivation paths have been estimated in the previous study,[12] a more accurate determination of these barriers is crucial to quantitatively understand the ultrafast excited-state dynamics in 9H-adenine, which is the primary goal of this study.

TABLE 1: Calculated Lowest Singlet-State Vertical Excitation Energies for 9H-Adenine[a]

	vertical excitation energy (eV)			
	this work	other theoretical values		expt
state	CASPT2[b]	CASPT2[c]	TD-DFT[d]	
$^1\pi\pi^*$ (^1L_b)	4.754 (0.002)	4.852 (0.006)	5.08 (0.167)	4.59[e,f], 4.63[g]
$^1\pi\pi^*$ (^1L_a)	4.879 (0.329)	4.902 (0.142)	5.35 (0.065)	4.92[h]
$^1n\pi^*$	4.995 (0.007)	5.503 (0.004)	4.97 (0.000)	
$^1n\pi^*$	5.626 (0.005)	5.685 (0.006)		

[a] Oscillator strengths are in parentheses. [b] The ground-state geometry is optimized by B3LYP/6-311G* method. [c] Ref 12. [d] Ref 16. [e] Ref 18. [f] Ref 19. [g] Ref 20. [h] Ref 21, in gas phase.

Here, we will report our CASPT2 results with a larger active space and basis set. The employed basis set is 6-311G* of polarized triple-ζ quality throughout this work. Unless stated otherwise, the active space is up to 14 electrons distributed in 11 orbitals, which consists of 2 lone pairs of nitrogen atoms in the pyrimidine ring and 9 π orbitals. The geometry optimizations for stationary points and CIs were performed with the *Gaussian 03* program.[14] The CASPT2 energy calculations were performed with MOLPRO software.[15]

The computed spectroscopic properties are compiled in Table 1. The calculated vertical excitation energies are in agreement with the experimental values. The vertical excitation energy of the lowest $^1n\pi^*$ excited state is predicted to be 4.995 eV, which agrees well with the a previous TD-DFT result.[16] However, previous CASPT2 calculations suggested that the lowest $^1n\pi^*$ excited state is about 0.7[12] and 1 eV[17] higher than the lowest

* shuhua@nju.edu.cn.

10.1021/jp0537207 CCC: $30.25

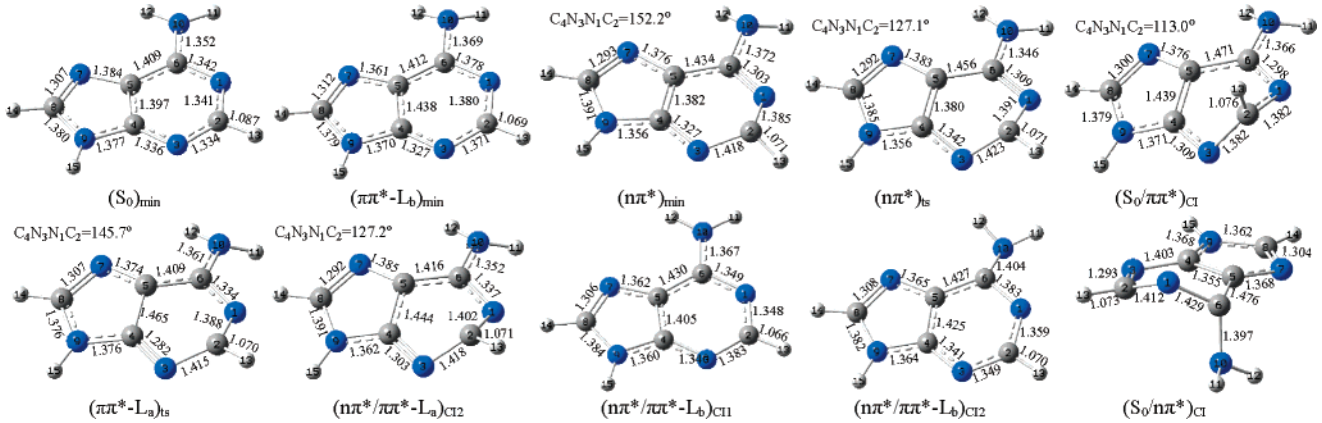

Figure 1. The structures of the CASSCF optimized minima, transition states, and conical intersections.

$^1\pi\pi^*$ excited state. This is probably because, in the previous CASPT2 calculations, only one lone pair of a nitrogen atom in the pyrimidine ring is included in the active space. Our results here indicated that the inclusion of the two lone pairs of the nitrogen atoms in the pyrimidine ring is very important for obtaining the accurate vertical excitation energy of the lowest $^1n\pi^*$ excited state. Correspondingly, the use of a small active space without including the two lone pairs could lead to large uncertainty in the estimate of the barrier associated with the $^1\pi\pi^*/^1n\pi^*$ transition near the Franck−Condon region, which is the first step in the nonradiative deactivation of 9H-adenine.

On the lowest $^1\pi\pi^*$ and $^1n\pi^*$ excited-state surfaces, two minima $(\pi\pi^*-L_b)_{min}$ and $(n\pi^*)_{min}$ in the Franck−Condon region were located through the CASSCF method, which have similar structures as determined previously.[12] As shown in Figure 1, the structure of $(n\pi^*)_{min}$ is slightly pyramidalized at the C_2 atom. The structure of $(\pi\pi^*-L_b)_{min}$ is nearly planar, except for the slight pyramidalization of the N_{10} atom in the amino group. The CASPT2 energy-level sequence of these two states at the geometry of one minimum is opposite that at the geometry of another minimum. This indicates the existence of a $^1n\pi^*/^1\pi\pi^*$ CI between these two minima, which is responsible for the transition from $^1\pi\pi^*$ (^1L_b) to $^1n\pi^*$. From Figure 1, one can see that the geometry of this CI, labeled $(n\pi^*/\pi\pi^*-L_b)_{CI1}$, is planar, being different from the structure obtained previously, where the C_2 atom is pyramidalized.[12] On the basis of the linearly interpolated internal coordinates (LI−IC) between $(\pi\pi^*-L_b)_{min}$ and $(n\pi^*/\pi\pi^*-L_b)_{CI1}$ (see Figure SI2 in Supporting Information), the barrier for crossing this $^1\pi\pi^*/^1n\pi^*$ transition is found to be 2.51 kcal/mol at the CASPT2 level. (The barrier height estimated in this way should be understood as an upper bound to a real barrier over a saddle point on a particular pathway.)

The LI−IC path between the ground-state equilibrium geometry $(S_0)_{min}$ and $(\pi\pi^*-L_b)_{min}$ indicates that after excitation to $^1\pi\pi^*$ (^1L_b) the system could spontaneously relax to $(\pi\pi^*-L_b)_{min}$ without any barrier (see Figure SI1 in Supporting Information). Along this LI−IC path, we found from CASPT2 calculations that there exists a CI labeled $(n\pi^*/\pi\pi^*-L_a)_{CI1}$ between $^1\pi\pi^*$ (^1L_a) and $^1n\pi^*$, which corresponds to the transition from $^1\pi\pi^*$ (^1L_a) to $^1n\pi^*$. We notice that this CI could not be located at the CASSCF level. The relaxation of the system from the Franck−Condon region to $(n\pi^*/\pi\pi^*-L_a)_{CI1}$ on the $^1\pi\pi^*$ (^1L_a) surface does not need extra energy input, implying that the transition from $^1\pi\pi^*$ (^1L_a) to $^1n\pi^*$ should happen easily.

At the CASSCF(14, 11) level, the optimized structure of the CI, $(S_0/\pi\pi^*)_{CI}$, between the ground state and S_1, is shown in Figure 1. This structure is qualitatively similar to that determined previously.[12] Along the LI−IC path between $(n\pi^*)_{min}$ and $(S_0/\pi\pi^*)_{CI}$, one can see that there exists a transition state (TS) from $(n\pi^*)_{min}$ to $(S_0/\pi\pi^*)_{CI}$ (see Figure SI4 in Supporting Information). We successfully located this TS, labeled $(n\pi^*)_{ts}$, as shown in Figure 1. The subsequent CASPT2 calculations lead to a barrier of 3.15 kcal/mol (with ZPE correction). This result differs significantly from the previous result, where the barrier disappeared at the CASPT2 level.[12] Interestingly, we noticed that the electronic character of the S_1 state changes from $n\pi^*$ to $\pi\pi^*$ when the system leaves from the transition state, $(n\pi^*)_{ts}$, to reach the CI, $(S_0/\pi\pi^*)_{CI}$. To elucidate how this change happens, we calculated the energies of the $^1\pi\pi^*$ (^1L_b) and $^1\pi\pi^*$ (^1L_a) states along the LI−IC path between $(n\pi^*)_{min}$ and $(S_0/\pi\pi^*)_{CI}$ (see Figure SI4 in Supporting Information). The results show that the $^1\pi\pi^*$ (^1L_a) state should involve in the $n\pi^*/\pi\pi^*$ transition from $(n\pi^*)_{ts}$ to $(S_0/\pi\pi^*)_{CI}$. We successfully located a CI between the $^1\pi\pi^*$ (^1L_a) state and the lowest $^1n\pi^*$ state, labeled $(n\pi^*/\pi\pi^*-L_a)_{CI2}$. As seen from Figure 1, the structure of $(n\pi^*/\pi\pi^*-L_a)_{CI2}$ is similar to those of $(n\pi^*)_{ts}$ and $(S_0/\pi\pi^*)_{CI}$ in that the C_2 atom in all three of these species is bending out of the plane. The bending dihedral angle $\delta(C_4N_3N_1C_2)$ is 127.2° in $(n\pi^*/\pi\pi^*-L_a)_{CI2}$, whereas it is 127.1° in $(n\pi^*)_{ts}$ and 113.0° in $(S_0/\pi\pi^*)_{CI}$. The calculated energy of $(n\pi^*/\pi\pi^*-L_a)_{CI2}$ is about 1.3 kcal/mol higher than that of $(n\pi^*)_{ts}$, but it is 1.9 kcal/mol lower than the vertical excitation energy of the $^1\pi\pi^*$ (^1L_a) state at the CASPT2 level. Clearly, the identification of this $n\pi^*/\pi\pi^*-L_a$ CI answers the questions why and how the S_1 state changes from $n\pi^*$ character to $\pi\pi^*$ character.

We successfully located a transition state on the $^1\pi\pi^*$ (^1L_a) surface, labeled $(\pi\pi^*-L_a)_{ts}$, through which the system could evolve from the Franck−Condon region to $(n\pi^*/\pi\pi^*-L_a)_{CI2}$. As shown in Figure 1, the structure of $(\pi\pi^*-L_a)_{ts}$ is similar to that of $(n\pi^*/\pi\pi^*-L_a)_{CI2}$ except that the dihedral angle $\delta(C_4N_3N_1C_2)$ is significantly larger in $(\pi\pi^*-L_a)_{ts}$. This indicates that the geometry relaxation mainly consists of the out-of-plane bending of the C_2 atom during the process from $(\pi\pi^*-L_a)_{ts}$ to $(n\pi^*/\pi\pi^*-L_a)_{CI2}$. The calculated energy of $(\pi\pi^*-L_a)_{ts}$ is 4.25 kcal/mol higher than the vertical excitation energy of the $^1\pi\pi^*$ (^1L_a) state at the CASPT2 level. So, our results suggest that a low barrier must be overcome for the system to reach $(n\pi^*/\pi\pi^*-L_a)_{CI2}$ on the $^1\pi\pi^*$ (^1L_a) surface, whereas a barrierless process was suggested for this step from the previous study.[12]

The deactivation path from the Franck−Condon region of several low-lying singlet excited states to $(S_0/\pi\pi^*)_{CI}$ can be summarized in Figure 2 (path a). First, the $^1n\pi^*$ state decreases in energy to cross with the $^1\pi\pi^*$ (^1L_a) and $^1\pi\pi^*$ (^1L_b) states sequentially toward the minimum $(n\pi^*)_{min}$ on the $^1n\pi^*$ surface. Then, the system must go through the transition state $(n\pi^*)_{ts}$ with a barrier of 3.15 kcal/mol to reach $(S_0/\pi\pi^*)_{CI}$. Along the

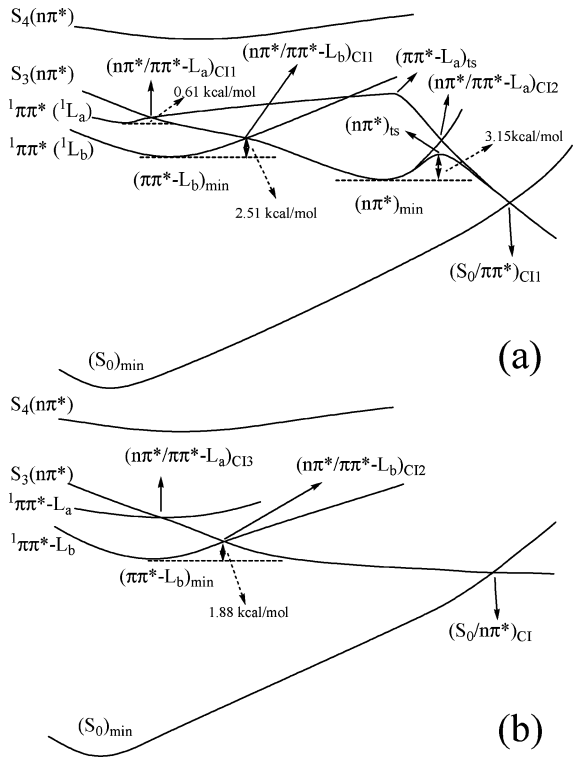

Figure 2. The nonradiative deactivation paths for singlet excited states of 9H-adenine: (a) to $(S_0/\pi\pi^*)_{CI}$; (b) to $(S_0/n\pi^*)_{CI}$.

$^1\pi\pi^*$ (^1L_a) surface, the system could go through the transition state $(\pi\pi^*-L_a)_{ts}$ to reach $(n\pi^*/\pi\pi^*-L_a)_{CI2}$ and then decay to the ground state through $(S_0/\pi\pi^*)_{CI}$. As shown in Figure 2, there is another path, labeled (b), through which the excited 9H-adenine can also deactivate to the ground state. We will give a brief discussion on the results for this path below.

First, a CI between the lowest $^1n\pi^*$ state and the ground state, labeled $(S_0/n\pi^*)_{CI}$, was successfully determined at the CASSCF-(14,11) level. This CI was determined previously using a smaller active space[12] and was proposed to account for the nonradiative deactivation from the lowest $^1n\pi^*$ state to the ground state. The structure of this CI (shown in Figure 1) is characterized by bending of the amino group and pyramidalization at the C_6 and N_1 atoms.

Our CASSCF optimization also led to a CI, labeled $(n\pi^*/\pi\pi^*-L_b)_{CI2}$, which provides another path for the transition from the $^1\pi\pi^*$ (^1L_b) state to the lowest $^1n\pi^*$ state (this CI is different from $(n\pi^*/\pi\pi^*-L_b)_{CI1}$ in Figure 2a). This CI was not found in the previous study.[12] At this CI, the amino group of 9H-adenine is bending out of the plane so that there is slight pyramidalization at the C_6 atom. The CASPT2 calculations along the LI−IC path between $(S_0)_{min}$ and $(n\pi^*/\pi\pi^*-L_b)_{CI2}$ indicate that the barrier to cross $(n\pi^*/\pi\pi^*-L_b)_{CI2}$ is 1.88 kcal/mol (see Figure SI5 in Supporting Information). Along this LI−IC path, we also found a CI between $^1\pi\pi^*$ (^1L_a) and $^1n\pi^*$, labeled $(n\pi^*/\pi\pi^*-L_a)_{CI3}$, which provides a path for the $\pi\pi^*-L_a/n\pi^*$ transition. This CI is absent at the CASSCF level, similar to $(n\pi^*/\pi\pi^*-L_a)_{CI1}$. The transition from $^1\pi\pi^*$ (^1L_a) to $^1n\pi^*$ through $(n\pi^*/\pi\pi^*-L_a)_{CI3}$ is calculated to be barrierless.

To conclude, along path (b) the $^1n\pi^*$ state will cross to $^1\pi\pi^*$ (^1L_a) through $(n\pi^*/\pi\pi^*-L_a)_{CI3}$ and to $^1\pi\pi^*$ (^1L_b) through $(n\pi^*/\pi\pi^*-L_b)_{CI2}$. After these crossings, the energy of the $^1n\pi^*$ state decreases all the way to the CI, $(S_0/n\pi^*)_{CI}$ (see Figure SI6 in Supporting Information). Thus, the results of both paths indicate that the $^1n\pi^*$ state is involved in ultrafast deactivation from the $^1\pi\pi^*$ (^1L_b) or $^1\pi\pi^*$ (^1L_a) state.

On the basis of the results described above, we proposed the following explanation for the experimentally found significant excitation−energy dependence of the excited-state lifetime in the gas phase.[9] First, on 250 nm excitation, the $^1\pi\pi^*$ (^1L_a) state is likely to be populated. From paths (a) and (b) in Figure 2, it can be seen that the transition from $^1\pi\pi^*$ (^1L_a) to $^1n\pi^*$ involves very low barriers (even no barriers). This result may account for the short (<50 fs) lifetime of the $^1\pi\pi^*$ excited state. The deactivation of $^1n\pi^*$ in path (a) to reach $(S_0/\pi\pi^*)_{CI}$ with a barrier of 3.15 kcal/mol might be responsible for the 750 fs lifetime of the $^1n\pi^*$ excited state. Second, on 267 nm excitation, the lower $^1\pi\pi^*$ (^1L_b) state with higher vibrational levels may be populated. Vibrationally active $^1\pi\pi^*$ (^1L_b) molecules can readily overcome the barriers needed for the transition to $^1n\pi^*$. Thus, the short (<50 fs) lifetime of the $^1\pi\pi^*$ excited state on 267 nm excitation could also be explained. At last, for the near-band origin of 277 nm excitation, 9H-adenine can only be excited to its $^1\pi\pi^*$ (^1L_b) state without much excessive vibrational energy. Because of the existence of the low barriers for $^1\pi\pi^*$ (^1L_b) to reach two CIs, $(S_0/\pi\pi^*)_{CI}$ and $(S_0/n\pi^*)_{CI}$ in paths (a) and (b), respectively, the deactivation of the $^1\pi\pi^*$ (^1L_b) state would take a relatively long time, which is in agreement with the observed >2 ps lifetime. The observed strong coupling between the $^1n\pi^*$ and $^1\pi\pi^*$ excited states[9] is also supported by the five CIs between the two $^1\pi\pi^*$ excited states and the lowest $^1n\pi^*$ excited state found in the current work.

Acknowledgment. This work was supported by the National Natural Science Foundation of China (grants 20373022 and 20233020) and Fok Ying Tong Education Foundation (grant 91014). We thank Virtual Laboratory for Computational Chemistry and Supercomputing Center, Computer Network Information Center, Chinese Academy of Sciences, for providing us with its computer facilities.

Supporting Information Available: Computational details, calculated energies, Cartesian coordinates of all stationary points and crossing points, and LI−IC results. This material is available free of charge via the Internet at http://pubs.acs.org.

References and Notes

(1) Callis, P. R. *Annu. Rev. Phys. Chem.* **1983**, *34*, 329.

(2) Crespo-Hernandez, C. E.; Cohen, B.; Hare, P. M.; Kohler, B. *Chem. Rev.* **2004**, *104*, 1977.

(3) Pecourt, J.-M. L.; Peon, J.; Kohler, B. *J. Am. Chem. Soc.* **2000**, 122, 9348.

(4) Pecourt, J.-M. L.; Peon, J.; Kohler, B. *J. Am. Chem. Soc.* **2001**, *123*, 10370.

(5) Peon, J.; Zewail, A. H. *Chem. Phys. Lett.* **2001**, *348*, 255.

(6) Cohen, B.; Hare, P. M.; Kohler, B. *J. Am. Chem. Soc.* **2003**, *125*, 13594.

(7) (a) Gustavsson, T.; Sharonov, A.; Markovitsi, D. *Chem. Phys. Lett.* **2002,** *351*, 195. (b) Gustavsson, T.; Sharonov, A.; Onidas, D.; Markovitsi, D. *Chem. Phys. Lett.* **2002,** *356*, 49.

(8) (a) Kang, H.; Lee, K. T.; Jung, B.; Ko, Y. J.; Kim, S. K. *J. Am. Chem. Soc.* **2002**, *124*, 12958. (b) Kang, H.; Jung, B.; Kim, S. K. *J. Chem. Phys.* **2003,** *118*, *6717*.

(9) Ullrich, S.; Schultz, T.; Zgierski, M. Z.; Stolow, A. *J. Am. Chem. Soc.* **2004**, *126*, 2262.

(10) (a) Ismail, N.; Blancafort, L.; Olivucci, M.; Kohler, B.; Robb, M. A. *J. Am. Chem. Soc.* **2002**, *124*, 6818. (b) Blancafort, L.; Robb, M. A. *J. Phys. Chem. A* **2004,** *108*, 10609.

(11) Merchán, M.; Serrano-Andrés, L. *J. Am. Chem. Soc.* **2003**, *125*, 8108.

(12) Perun, S.; Sobolewski, A. L.; Domcke, W. *J. Am. Chem. Soc.* **2005**, *127*, 6257.

(13) Marian, C. M. *J. Chem. Phys.* **2005,** *122*, 104314.

(14) Frisch, M. J.; Trucks, G. W.; Schlegel, H. B.; Scuseria, G. E.; Robb, M. A.; Cheeseman, J. R.; Montgomery, J. A., Jr.; T. V.; Kudin, K. N.; Burant, J. C.; Millam, J. M.; Iyengar, S. S.; Tomasi, J.; Barone, V.; Mennucci, B.; Cossi, M.; Scalmani, G.; Rega, N.; Petersson, G. A.; Nakatsuji, H.; Hada, M.; Ehara, M.; Toyota, K.; Fukuda, R.; Hasegawa, J.; Ishida, M.; Nakajima, T.; Honda, Y.; Kitao, O.; Nakai, H.; Klene, M.; Li, X.; Knox, J. E.; Hratchian, H. P.; Cross, J. B.; Adamo, C.; Jaramillo, J.; Gomperts, R.; Stratmann, R. E.; Yazyev, O.; Austin, A. J.; Cammi, R.; Pomelli, C.; Ochterski, J. W.; Ayala, P. Y.; Morokuma, K.; Voth, G. A.; Salvador, P.; Dannenberg, J. J.; Zakrzewski, G.; Dapprich, S.; Daniels, A. D.; Strain, M. C.; Farkas, O.; Malick, D. K.; Rabuck, A. D.; Raghavachari, K.; Foresman, J. B.; Ortiz, J. V.; Cui, Q.; Baboul, A. G.; Clifford, S.; Cioslowski, J.; Stefanov, B. B.; Liu, G.; Liashenko, A.; Piskorz, P.; Komaromi, I.; Martin, R. L.; Fox, D. J.; Keith, T.; Al-Laham, M. A.; Peng, C. Y.; Nanayakkara, A.; Challacombe, M.; Gill, P. M. W.; Johnson, B.; Chen, W.; Wong, M. W.; Gonzalez, C.; Pople, J. A. *Gaussian 03*, Revision B.03; Gaussian, Inc.: Pittsburgh, PA, 2003.

(15) Amos, R. D.; Bernhardsson, A.; Berning, A.; Celani, P.; Cooper, D. L.; Deegan, M. J. O.; Dobbyn, A. J.; Eckert, F.; Hampel, C.; Hetzer, G.; Knowles, P. J.; Korona, T.; Lindh, R.; Lloyd, A. W.; McNicholas, S. J.; Manby, F. R.; Meyer, W.; Mura, M. E.; Nicklass, A.; Palmieri, P.; Pitzer, R.; Rauhut, G.; Schütz, M.; Schumann, U.; Stoll, H.; Stone, A. J.; Tarroni, R.; Thorsteinsson, T.; Werner, H.-J. MOLPRO, a package of ab initio programs, version 2000.1; University of Birmingham, U.K., 1999.

(16) Mennucci, B.; Toniolo, A.; Tomasi, J. *J. Phys. Chem. A* **2001**, *105*, 4749.

(17) Fülscher, M. P.; Serrano-Andrés, L.; Roos, B. O. *J. Am. Chem. Soc.* **1997**, *119*, 6168.

(18) Voelter, W.; Records, R.; Bunnenberg, E.; Djerassi, C. *J. Am. Chem. Soc.* **1968**, *90*, 6163.

(19) Matsuoka, Y.; Nordén, B. *J. Phys. Chem.* **1982**, *86*, 1378.

(20) Sutherland, J. C.; Griffin, K. *Biopolymers* **1984**, *23*, 2715.

(21) Clark, L. B.; Peschel, G. G.; Tinoco, I., Jr. *J. Phys. Chem.* **1965**, *69*, 3615.